Journal of Controlled Release 348 (2022) 786–797

Contents lists available at ScienceDirect

Journal of Controlled Release

journal homepage: www.elsevier.com/locate/jconrel

Lipid-peptide nanocomplexes for mRNA delivery *in vitro* and *in vivo*

Dania Grant-Serroukh [a,b], Morag R. Hunter [c], Ruhina Maeshima [a], Aristides D. Tagalakis [a,1], Ahmad M. Aldossary [a,2], Nour Allahham [b], Gareth R. Williams [b], Mark Edbrooke [c], Arpan Desai [c], Stephen L. Hart [a,*]

[a] UCL Great Ormond Street Institute of Child Health, University College London, 30 Guilford Street, London WC1N 1EH, UK
[b] UCL School of Pharmacy, University College London, 29 – 39 Brunswick Square, London WC1N 1AX, UK
[c] Pharmaceutical Sciences, AstraZeneca, Aaron Klug Building, Granta Park, Cambridge CB21 6GH, UK

ARTICLE INFO

Keywords:
mRNA
Transfection
Nanocomplexes
Lipids
Peptides
Targeting

ABSTRACT

Despite recent advances in the field of mRNA therapy, the lack of safe and efficacious delivery vehicles with pharmaceutically developable properties remains a major limitation. Here, we describe the systematic optimisation of lipid-peptide nanocomplexes for the delivery of mRNA in two murine cancer cell types, B16-F10 melanoma and CT26 colon carcinoma as well as NCI-H358 human lung bronchoalveolar cells. Different combinations of lipids and peptides were screened from an original lipid-peptide nanocomplex formulation for improved luciferase mRNA transfection *in vitro* by a multi-factorial screening approach. This led to the identification of key structural elements within the nanocomplex associated with substantial improvements in mRNA transfection efficiency included alkyl tail length of the cationic lipid, the fusogenic phospholipid, 1,2-dioleoyl-*sn*-glycero-3-phosphoethanolamine (DOPE), and cholesterol. The peptide component (K_{16}GACYGLPHKFCG) was further improved by the inclusion of a linker, RVRR, that is cleavable by the endosomal enzymes cathepsin B and furin, and a hydrophobic motif (X-S-X) between the mRNA packaging (K_{16}) and receptor targeting domains (CYGLPHKFCG). Nanocomplex transfections of a murine B16-F10 melanoma tumour supported the inclusion of cholesterol for optimal transfection *in vivo* as well as *in vitro*. *In vitro* transfections were also performed with mRNA encoding interleukin-15 as a potential immunotherapy agent and again, the optimised formulation with the key structural elements demonstrated significantly higher expression than the original formulation. Physicochemical characterisation of the nanocomplexes over time indicated that the optimal formulation retained biophysical properties such as size, charge and mRNA complexation efficiency for 14 days upon storage at 4 °C without the need for additional stabilising agents. In summary, we have developed an efficacious lipid-peptide nanocomplex with promising pharmaceutical development properties for the delivery of therapeutic mRNA.

1. Introduction

Messenger RNA (mRNA) therapy is fast becoming one of the most promising modalities in gene therapy as it offers opportunities to treat disease by using the cells natural processes to replace or augment protein production [1]. Most notably, mRNA lipid nanoparticles (LNPs) expressing SARS-CoV-2 spike (S) protein, were rapidly developed and deployed as vaccines for COVID-19 [2]. In addition to protein-replacement therapies for monogenic diseases or as vaccines, therapeutic mRNA in protein expression offers opportunities in CRISPR-based gene-editing, where mRNA provides an approach to guide RNA-targeted delivery of the Cas9 nuclease to knock-out genes to treat diseases, such as transthyretin amyloidosis (ATTR) [3–5]. Key advantages of mRNA over DNA-based modalities include, i) increased transfection efficiency of mRNA compared to plasmid DNA (pDNA), which requires nuclear transcription where the nuclear envelope represents a major barrier in post-mitotic cells. Messenger RNA need only be delivered to the cytoplasm where it can engage with the ribosomal machinery for protein translation; ii) greater safety and control of expression as mRNA is less persistent than pDNA, and; iii) reduced risk of genotoxicity as mRNA cannot integrate into chromosomal DNA, and, iv) ease of manufacture of mRNAs by enzymatic, *in vitro* transcription compared to bacterial

* Corresponding author.
E-mail address: s.hart@ucl.ac.uk (S.L. Hart).
[1] Current address: Department of Biology, Edge Hill University, Ormskirk, L39 4QP, UK.
[2] Current address: National Centre for Biotechnology, King Abdulaziz City for Science and Technology, Riyadh 11442, Saudi Arabia.

https://doi.org/10.1016/j.jconrel.2022.06.018
Received 8 February 2022; Received in revised form 30 May 2022; Accepted 10 June 2022

fermentation and extraction for pDNA, with extensive purification required [1].

A key bottleneck in the development of mRNA therapeutics is its safe and effective delivery, particularly *in vivo*. There are several challenges which must be addressed to achieve this; firstly, the mRNA must be protected from degradation by extracellular ribonucleases, then the formulation should target the affected tissue where it must enter the cells by endocytosis, and escape the endosome to avoid degradation, and release the mRNA cargo into the cytoplasm. Messenger RNA is a large, negatively-charged molecule which largely precludes it from cellular entry across the hydrophobic lipid bilayer of the cell membrane and so a carrier is required, and non-viral, nanoparticle formulations offer a particularly promising route to achieve this. To address this delivery bottleneck, we focus in this study on developing a novel, self-assembling nanocomplex formulation for mRNA delivery.

A diverse array of formulations for mRNA delivery have been reported [6], such as LNPs [7,8] and polymers [9]. Lipid-hybrid formulations, which amalgamate lipids with polymers or peptides may prove to be more effective than lipids alone by providing additional functionality to the lipocomplexes to enable them to overcome cellular barriers more effectively, such as cell entry and endosomal escape [10,11]. While mRNA shares some fundamental biological barriers to delivery as pDNA, there are marked chemical and structural differences which will affect the electrostatic self-assembly processes. For example, pDNA is a circular, double-stranded DNA molecule, typically of 5–10 kb depending on the size of the encoded gene, with a double-stranded, supercoiled DNA 3D structure. Messenger RNA molecules are single-stranded, linear RNA of approximately 1 or more kb that form extensive secondary structures, so they occupy very different dimensions in solution to pDNA [1]. Lipocomplexes of mRNA and lipids, such as LNPs, have proven effective as transfection agents for short interfering RNA (siRNA), which are linear, double stranded RNA molecules of 20–23 nt, but may not be optimal for mRNA delivery. For example, the potency of an LNP mRNA formulation, developed originally for siRNA delivery, increased 7-fold *in vivo* by optimising the formulation [12].

We have previously described a multifunctional, lipid-peptide nanocomplex that consists of a mixture of lipids and peptides that complex electrostatically with nucleic acids including pDNA and siRNA. The formulation comprises cationic lipids such as DOTMA, helper lipids such as DOPE, which provide fusogenic properties to facilitate endosomal escape, and peptides, consisting of a positively-charged oligolysine motif, for electrostatic binding to mRNA, and a targeting motif for receptor-targeted uptake [10]. Lipid-peptide formulations have proven to be effective for plasmid DNA (pDNA) [13] and siRNA delivery [14], but the suitability of this system for mRNA delivery has not yet been determined.

The aim of this work was to optimise the lipid-peptide delivery system for mRNA delivery and evaluate its efficacy *in vitro* and *in vivo*. We hypothesised that altering the components and composition of the system to account for differences between mRNA and other nucleic acids, could improve potency. Each lipid and peptide component of the system was optimised systematically by multifactorial screening. Formulations were assessed *in vitro* in consecutive luciferase mRNA transfection screens, with the best performers being taken forward at each stage. In this study we have elucidated some unique characteristics of mRNA nanoformulations, including the role of cholesterol, that may contribute to the further development of mRNA-based therapeutics.

2. Methods

2.1. Liposome preparation

The cationic lipids used were ditetradecyl trimethyl ammonium propane (DTDTMA), dihexadecenyl trimethyl ammonium propane (DHDTMA) or dioctadecenyl trimethyl ammonium propane (DOTMA) which are referred to as C14, C16 and C18 respectively to indicate the length of their respective alkyl chains. Cationic lipids were mixed with one of the following phospholipids: 1,2-dioleoyl-*sn*-glycero-3-phosphoethanolamine (DOPE), 1,2-distearoyl-*sn*-glycero-3-phosphocholine (DSPC) or 1,2-dioleoyl-*sn*-glycero-3-phosphocholine (DOPC) at a 1:1 M ratio. All cationic lipids and phospholipids were purchased from Avanti Polar Lipids (Birmingham, AL, USA) and cholesterol from Sigma-Aldrich (Gillingham, UK). All lipid structures are shown in Table 1.

Liposomes were made using a Nanoassemblr microfluidic based system (Precision Nanosystems, Vancouver, BC, Canada). The cationic lipid and phospholipid were mixed at a 1:1 M ratio in ethanol and injected into the cartridge at a flow rate of 12 mL/min. Where cholesterol was added to the mixture, the molar concentration of cationic lipid remained constant at 50% and the ratio of phospholipid to cholesterol varied to give a specified molar percentage of cholesterol. The resulting liposomes were dialysed overnight in cellulose tubing (10 k MWCO) to remove any residual ethanol. They were then sonicated in a water bath for 20 min before being filtered through a 0.45 μm filter and dialysed overnight.

2.2. Peptides

All peptides were obtained from AMS Bio (Abingdon, UK) (Table 2). The peptides used to formulate nanocomplexes all contain K_{16} motifs for mRNA packaging plus targeting motifs and different linkers. Other key features include the RGD motif targeting motif in Peptide 27, while the other peptides contain the epithelial targeting motif (YGLPHKF), isolated by biopanning of a phage display peptide library on epithelial cells [15]. Both targeting motifs are flanked by cysteine residues to enable disulphide bridge cyclisation. Other key features include the spacer elements which include -GA, the furin or cathepsin B cleavable linker RVRR [16] and the hydrophobic linker, -XSX-, where X is the synthetic hydrophobic amino acid, ε-amino hexanoic acid.

2.3. Nanocomplex preparation

Nanocomplexes were prepared by mixing aqueous suspensions of liposomes, with solutions of peptides and mRNA (Table S1). Firefly luciferase mRNA (5-methylcytidine, pseudouridine; FLuc mRNA [5meC, Ψ]), was purchased from TriLink Biotechnologies (San Diego, CA, USA). The complexes were prepared to a final mRNA concentration of 0.5 μg/mL by mixing in the order of mRNA (R), followed by the liposomes (L), and finally the peptides (P). The components were added at weight ratios of 1:3:4 (R:L:P respectively), unless otherwise stated. The components were mixed in OptiMEM (Thermo-Fisher Scientific, Paisley, UK) and incubated at room temperature for 30 min for the nanocomplexes to stabilise before being used for transfection experiments.

2.4. Nanocomplex physical characterisation

The size and charge of the complexes was determined using a Nano ZS zetasizer (Malvern Instruments, Malvern, UK). Complexes were made as described for transfections, except that the complexes were formed in water rather than OptiMEM, and at a higher mRNA concentration of 1 μg/mL. Intensity measurements were taken in triplicate and the z-average particle sizes recorded.

Efficiency of mRNA complexation was measured by calculating the percentage of free mRNA after formation of the nanocomplexes. RiboGreen reagent (Thermo Fisher Scientific, Paisley, UK) was mixed with 1 x Tris-EDTA buffer (pH 8) at a 1:200 *v*/v ratio using a vortex and incubated for 5 min at room temperature. The RiboGreen-labelled mRNA was formulated into nanocomplexes as described above for transfection experiments, except with the substitution of OptiMEM for water. Fluorescence was analysed using a FLUOstar Optima fluorescence plate reader (BMG Labtech, Aylesbury, UK). Free mRNA stained with RiboGreen was used to normalize the RiboGreen signal detected from the complexes.

Table 1
Lipids used in this study. DOPE - 1,2-dioleoyl-*sn*-glycero-3-phosphoethanolamine, **DSPC** - 1,2-distearoyl-sn-glycero-3-phosphocholine; **DOPC -**,2-Dioleoyl-sn-glycero-3-phosphocholine. **DOTMA** (C18) - 1,2-Di-((*Z*)-octadec-9-enyloxy)-*N,N,N* trimethylammonium propane chloride; **DHDTMA** (C16) - 1,2-Di-((*Z*)-hexadec-11-enyloxy)-*N,N,N* trimethylammonium propane iodide and **DTDTMA** (C14) - 1,2-Di-((*Z*)-tetradec-11-enyloxy)-*N,N,N* trimethylammonium propane chloride; **Cholesterol (**Chol).

Lipid	Structure	Molecular weight (Da)
DOPE	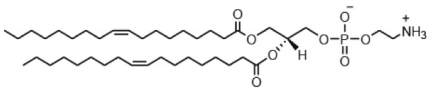	744.03
DSPC	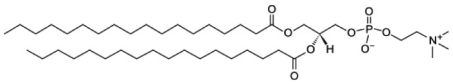	790.15
DOPC	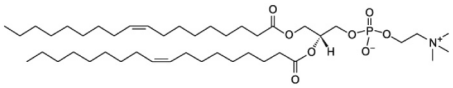	786.11
DOTMA (C18	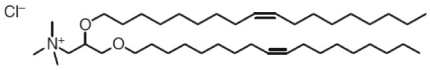	670.58
DHDTMA (C16)	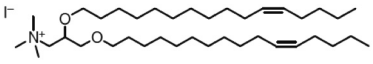	614.47
DTDTMA (C14)	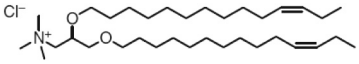	558.36
Cholesterol (Chol)	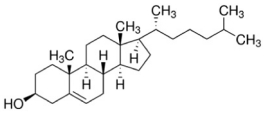	386.66

Table 2
Peptides used in this study.

NAME	SEQUENCE	Molecular weight (Da)
Peptide 27	K_{16}RVRRGACRGDCLG	3469.5
Peptide 28	K_{16}GACYGLPHKFCG	3303.3
Peptide 31	K_{16}XSXGACYGLPHKFCG	3616.7
Peptide 32	K_{16}RVRRGACYGLPHKFCG	3871.0
Peptide 35	K_{16}RVRRXSXGACYGLPHKFCG	4184.4

2.5. In vitro cell culture and transfection

B16-F10-AP3 murine melanoma cells (B16-F10) were kindly provided by AstraZeneca. Human lung epithelial (H358) and mouse colon fibroblast (CT26.WT) cells were obtained from ATCC through LGC (Teddington, UK). B16-F10 cells were grown in Dulbecco's Modified Eagle Medium with high glucose (Sigma Aldrich, Gillingham, UK), supplemented with 10% *v*/v foetal calf serum (Thermo Fisher Scientific, Paisley, UK) and GlutaMAX-I (Thermo Fisher Scientific, Paisley, UK). CT26 and H358 cells were grown in RPMI (Sigma Aldrich, Gillingham, UK), supplemented with 10% v/v foetal calf serum and Glutamax. All cell lines were grown in a humidified 5% CO_2 atmosphere at 37 °C.

For luciferase transfections, cells were seeded in white 96-well plates with clear bottoms at 20,000 cells/well for B16-F10 and H358 cells, and at 10,000 cells/well for CT26 cells to reach 70% confluence at the time of transfection, 24 h after seeding. Nanocomplexes were prepared as described above and added to cells and incubated at 37 °C in 5% CO_2 for 4 h, after which the medium containing the nanocomplexes was removed and replaced with culture media containing serum. The cells were incubated for a further 24 h at 37 °C before luciferase assays were performed. For EGFP mRNA transfection experiments, cells were seeded in clear 12-well plates, but otherwise the transfection procedure was as described above.

2.6. Cytotoxicity assay

The cytotoxicity of formulations was investigated using a CCK-8 kit (Sigma Aldrich, Gillingham, UK). This is a colorimetric assay that determines cell viability by measuring the reduction of a tetrazolium salt by the cellular dehydrogenase present in living cells. Lipofectamine 2000 (Thermo Fisher Scientific, Paisley, UK) was used as a control along with naked mRNA.

2.7. Transfection assays

24 h after transfection, cells were washed twice with PBS and levels of transfection were measured using a bioluminescent firefly luciferase assay (Promega, Southampton, UK). Cells were lysed by addition of 20 μL Reporter Lysis Buffer directly to the cells then left at 4 °C for 20 min, before transferring to -80 °C for rapid freezing and left at least 40 min. Plates were then thawed at room temperature to ensure complete cell lysis. Fifty microlitres of luciferase substrate from the luciferase assay system was added to each well. Luciferase activity was determined in a FLUOstar Optima plate reader (BMG Labtech). All results were normalised to total protein content using the Bradford protein assay reagent (Bio-Rad, Watford, UK) with the results expressed as relative luminescence units per milligram of protein (RLU/mg).

For the EGFP expression assay, cells were transfected with EGFP mRNA then detached using Trypsin-EDTA and resuspended in complete cell media in fluorescence-activated cell sorting (FACS) tubes. Cells were then sorted with a FACS Calibur flow cytometer (BD Biosciences, Wokingham, UK) and analysis was performed with FlowJo software v. 8.8.3.

An ordinary one-way analysis of variance analysis (ANOVA) followed by a Tukey's multiple comparison test was used to evaluate data obtained from transfection experiments. Means were considered significantly different when $p < 0.05$.

2.8. mRNA uptake assay

Cells were seeded in 96-well plates (CellCarrier Ultra, Perkin Elmer, Beaconsfield, UK) at 20,000 cells/well for B16-F10, 10,000 cells/well for CT26, and 20,000 cells/well for H358 cells. Transfections were performed by adding each formulation with 100 ng/well Cy5-labelled

GFP mRNA (Trilink Biotechnologies (San Diego, CA, USA) to the growth media at time points ranging from 24 h to 30 min such that all incubation times finished simultaneously. Samples were fixed in 4% paraformaldehyde, and nuclei were stained with Hoechst 33342 (Thermo Fisher Scientific, Paisley, UK) at 1:1000 dilution. Images were captured on a Yokogawa CV8000 automated confocal microscope (Yokogawa UK Ltd., Runcorn, UK), using a 60× water-immersion objective (numerical aperture 1.2). Images were analysed in Columbus (version 2.8.2, Perkin Elmer) and data analysed in Prism (versions 7 and 8, GraphPad). In brief, cell nuclei and cytoplasm were identified, and Cy5 mRNA fluorescence was measured in the total cell area (nucleus and cytoplasm). Cells were scored as positive for intracellular Cy5 if fluorescence was above background, defined by cells incubated with buffer only, on the same assay plate.

2.9. RNase degradation assay

Nanocomplexes were prepared in water and incubated for 30 min at room temperature to stabilise. 10 μg RNase (Generon, Slough, UK) was added to the samples which were then incubated at 37 °C for 30 min, after which 8 U of Ribolock RNase inhibitor (Thermo-Fisher Scientific, Paisley, UK) was added. The samples were then used in luciferase transfection experiments.

2.10. Gel retardation analysis

Gel retardation assays were performed by preparing luciferase mRNA nanocomplexes in water and either untreated (−) or treated (+) with 20 U/mL heparan sulphate for 1 h at room temperature then loaded onto a 1% agarose gel, made in Tris-Acetate-EDTA (TAE) buffer, pH 8.3, stained with 1 μg/mL ethidium bromide, and electrophoresed at a voltage of 100 V for 1 h with TAE as the running buffer.

2.11. In vivo studies

Female C57BL/6 J mice were purchased from Charles River (Margate, UK). All procedures were approved by UCL animal care policies and were carried out under Home Office licences issued in accordance with the United Kingdom Animals Scientific Procedures Act 1986. Mice were injected subcutaneously on the flank with 10,000 B16-F10 cells in a suspension containing 50:50 RPMI and Matrigel and observed daily for the development of tumours. Nanocomplexes were prepared as described above at an mRNA concentration of 0.2 mg/mL then 50 μL of the nanocomplex suspension was injected intratumorally. Control mice with tumours were left untreated. 24 h following injections, mice were culled, and tumours extracted, submerged in reporter gene assay lysis buffer (Thermo Scientific, Paisley, UK), homogenised with a tissue homogeniser, and centrifuged at 14,170 x *g* for 10 min at 4 °C, after which the supernatant was removed and centrifuged for a further 10 min at 4 °C before being used in the luciferase assay. Statistical analysis was performed by an ordinary one-way analysis of variance analysis (ANOVA) followed by a Tukey's multiple comparison test. Means were considered significantly different when $p < 0.05$.

2.12. Mouse IL-15 mRNA transfection and ELISA

B16-F10 cells were seeded at 1×10^5 cells per well in 6 well plates and incubated overnight in a humidified 5% CO_2 atmosphere at 37 °C. 1 mg murine IL-15 mRNA was obtained as a custom synthesis from TriLink using the sequence REFSEQ: accession NM_001254747.2 (Protein-NCBI; www. nih.gov) and formulated in nanocomplexes as described above. Six-well plates containing the cells and transfection mixes were centrifuged at 300 x *g* for 5 min to enhance transfection, then returned to the incubator for 4 h before replacing the transfection mix with complete medium. The medium containing secreted IL-15 was collected after 72 h and concentrated using Amicon Ultra (10,000 nominal molecular weight limit), 2 mL Centrifugal Filters (Millipore, Watford, UK) at 4000 x *g* for 20 min. Mouse IL-15 ELISA assay was performed using the mouse IL-15/IL-15R ELISA Kit (Thermo-Fisher Scientific, Paisley, UK) to detect secreted IL-15 protein according to the manufacturer's instructions.

2.13. Statistical analysis

Statistical analysis was performed by an ordinary one-way analysis of variance analysis (ANOVA) followed by a Tukey's multiple comparison test. Means were considered significantly different when $p < 0.05$.

3. Results

3.1. Optimisation of screening conditions

Preliminary experiments were designed to establish a narrow set of parameters which could be used to optimise nanocomplexes for mRNA delivery. Luciferase mRNA (R) transfections were performed with a formulation of cationic liposomes (L; DTDTMA(C14)/DOPE) and Peptide 27 (Fig. 1).

The term “nanocomplex” was chosen to differentiate the formulation from lipoplexes or LNP, which are typically formulations of cationic liposomes and nucleic acids, without peptides, or liposomes, which are the spherical lipid structures without nucleic acids or peptides.

We first investigated the effects of mixing order and component weight ratios, which indicated that formulations in which the peptide was added last (RLP and LRP), gave significantly higher levels of transfection ($p < 0.05$) (Fig. S1a). Although adding the peptide last was optimal in both B16-F10 and CT26 cell lines, optimal weight ratios of the components in the two cell lines were different. Formulations containing a higher proportion of cationic DTDTMA/DOPE liposome (3:1 L:R) transfected CT26 cells better than those containing a lower proportion (2:1 L:R), with all formulations containing a constant 4:1 ratio of P:R, whereas the opposite trend was observed with B16-F10 cells (Fig. S1b).

3.2. Multifactorial screens for transfection efficiency

In the first screen (Screen A), all three components of the system were varied (cationic lipids, phospholipids and peptides) (

Fig. 2). Three cationic lipids were selected with varying tail lengths (C14, C16 and C18), three phospholipids with different head groups or tail structures (DSPC, DOPE and DOPC) and five peptides with combinations of three linker designs and two types of targeting motif. Each combination of liposomes and peptide was formulated into nanocomplexes with luciferase mRNA at a constant weight ratio of 1:3:4 (R:L:

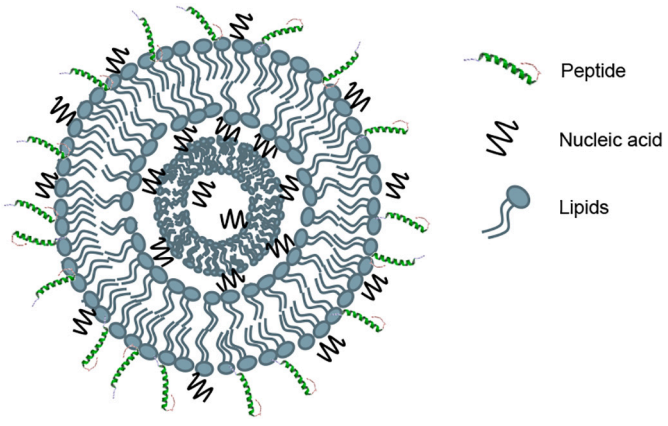

Fig. 1. Graphical representation of the lipid-peptide nanocomplex. Lipid-peptide nanocomplexes prepared by mixing mRNA with peptides and preformed liposomes comprising a 1:1 mol/mol composition of cationic lipids and phospholipids.

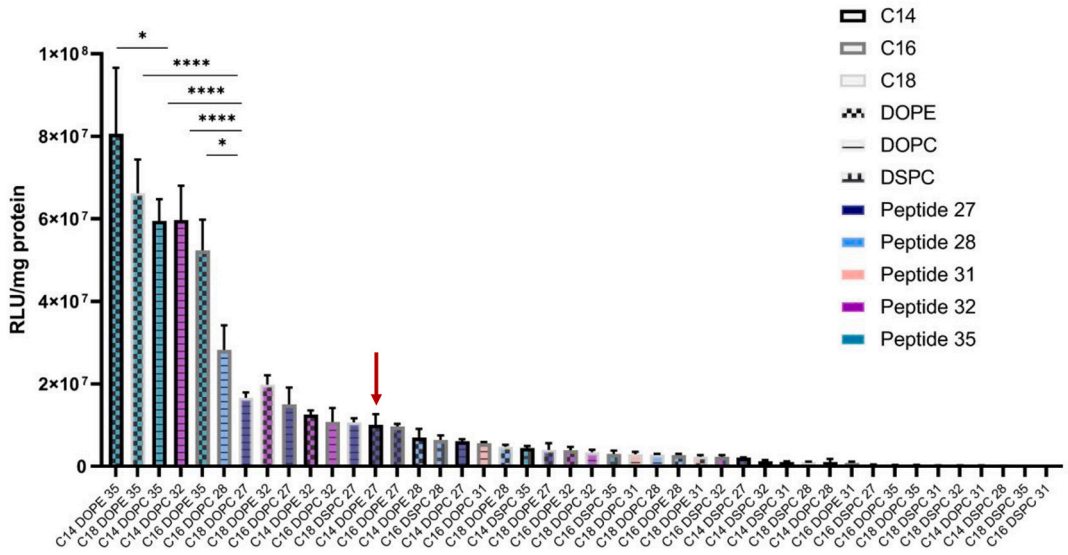

Fig. 2. Multifactorial screening of Lipid-Peptide nanocomplexes in mRNA luciferase transfections. Transfection efficiencies of formulations delivering 100 ng of mRNA with varying components at a constant weight ratio of 1 (mRNA): 3 (liposome): 4 (peptide) were compared in B16-F10 cells. Cationic lipids C14, C16 and C18 were screened with different phospholipids (DOPE, DSPC, DOPC) and peptides 27, 28, 31, 32, 35). Red arrow indicates the original formulation. DOPE-containing formulations produced higher protein expression than formulations containing DSPC or DOPC. Luciferase activity was measured in relative light units (RLU) per mg of protein 24 h after transfection. * indicates statistical significance where $p < 0.05$, and **** statistical significance where $p < 0.0001$, based on a one-way ANOVA test with Tukey post-hoc analysis. Data shown as mean ± SEM, $n = 6$. (For interpretation of the references to colour in this figure legend, the reader is referred to the web version of this article.)

P) and assessed for transfection efficiency in B16-F10 cells initially. Biophysical properties, including size, charge, percentage mRNA complexation, were determined (Table S2). All combinations resulted in particle sizes between 60 and 200 nm and all had encapsulation efficiencies >88%. There were no clear trends observed between physicochemical properties and the composition of the nanocomplexes (Table S2). Formulations including DOPE and peptide 35 performed better than other phospholipid/peptide combinations, with three of the top five formulations containing both components. Peptides containing a cleavable linker recognised by the enzymes furin and cathepsin B (peptides 27, 32 and 35), in general, performed better than those with either no linker (Peptide 28) or a hydrophobic linker (Peptide 31). No correlation was observed between the hydrocarbon chain length of the cationic lipid and transfection efficiency.

The impact on transfection efficiency of the phospholipids was DOPE>DOPC>DSPC. The optimal formulation from Screen A was C14/DOPE-Pep 35, with the comparative improvement reaching statistical significance ($p < 0.0001$) *vs* all formulations except C18/DOPE-Pep 35. This is an 8-fold improvement over the original C14/DOPE-Peptide 27 formulation optimised for siRNA and DNA delivery (8.06×10^7 *vs.* 1.01×10^7 RLU/mg protein). The transfection efficiency of formulations tested had a minimal effect on cell viability (Fig. S2) while those containing the C14 cationic lipid showed a slight but significant improvement to cell viability compared to those containing either C16 or C18 cationic lipids (Fig. S2a). All RLP formulations were less toxic than Lipofectamine 2000, which decreased cell viability by 30% relative to free mRNA.

We next evaluated inclusion of cholesterol into RLPs for its potential to increase transfection efficiency [17]. The molar percentage of cationic lipid was maintained at 50% while the cholesterol percentage was increased into the top five RLP formulations from 0 to 30% in screen B with a corresponding reduction of the helper lipid. The addition of 30% cholesterol significantly improved transfection efficiency in all DOPE-containing formulations and two DOPC-containing formulations, but this did not reach statistical significance in the latter (Fig. 3). Cell viability was not affected by the presence or absence of cholesterol (Fig. S3).

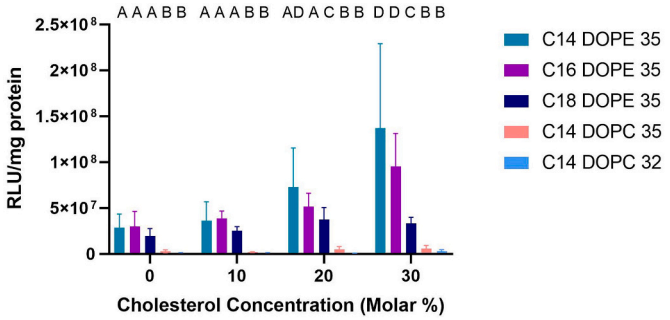

Fig. 3. The addition of cholesterol to DOPE formulations leads to an increased in reporter protein expression. Luciferase activity was measured in B16-F10 cells after transfection of 100 ng of mRNA with the top 5 formulations with the addition of cholesterol at molar ratios from 0 to 30%. Formulations which share a letter are not significantly different whilst those which do not are considered significantly different ($p < 0.05$) based on a one-way ANOVA with Tukey post-hoc analysis. Data shown as mean ± SEM, $n = 6$.

The composition C14/DOPE with peptide 35, and 30% cholesterol (C14/DOPE+30%chol-Pep35) produced the highest levels of transfected luciferase expression, an approximately 5–fold higher transfection efficiency compared to the equivalent formulation without cholesterol (1.37×10^8 compared with 2.87×10^7 RLU/mg protein) (Fig. 3). We then explored in Screen C whether any further improvement could be gained by altering the ratio of mRNA: liposome: peptide in a third screen (Fig. S4). A range of lipid/peptide compositions were investigated but, although better transfection was observed at higher lipid and/or peptide weight ratios, such as RLP at 1:4:5 containing C14/DOPE and C18/DOPE liposomes, this negatively impacted cell viability (Fig. S5). Formulations with the lowest proportions of lipid and peptide, such as RLP at 1:2:5, were the least cytotoxic although this was coupled with lower transfection efficiency. The mid-range RLP at 1:3:4, which was also used in screens A and B, was thus selected as the optimal formulation that gave mid-range transfection but with minimal cytotoxicity.

3.3. Comparison of transfections in different cell types

Screens A and B were then repeated on two additional cell lines, CT26 and H358, to assess the general application of this approach with lipid-peptide nanocomplexes. These screens showed that the same overall trends were observed across the cell types (Fig. 4). However, the degree of improvement appeared to be cell specific. This is particularly striking for nanocomplexes containing cholesterol, which show a greater improvement in transfection efficiency of the B16-F10 cell line (Fig. 4a), compared to the other cell types.

3.4. In vivo assessment of transfection

Some previous studies have suggested that there is only a weak correlation between nucleic acid transfection efficiency *in vitro* and *in vivo* [18,19], therefore, we investigated whether cholesterol enhanced transfection *in vivo,* in subcutaneous tumours established in the B16-F10 syngeneic mouse model. The lead nanocomplex (C14/DOPE+30%chol-Pep 35) was delivered by injection into the tumour and compared to the lead formulation from screen A which does not contain cholesterol (C14/DOPE-35). Untreated tumours were used as a negative control. Tumours were harvested after 24 h, and luciferase expression quantified (Fig. 5).

In concordance with *in vitro* experiments, the optimal cholesterol formulation produced significantly higher levels of protein expression than the formulation lacking cholesterol.

3.5. Investigations into enhanced transfection processes of cells

Improvements in luciferase mRNA transfection efficiency from the screening strategy could be attributed to more mRNA in transfected cells or an increased number of cells transfected and so to elucidate this we performed further transfections with mRNA encoding enhanced green fluorescent protein (eGFP), analysed in a flow cytometry assay. The optimal nanocomplex from screen B, C14/DOPE+30% Chol-Pep 35, was compared with its cholesterol-free counterpart in B16-F10 cells. There were no significant differences in the percentage of eGFP-positive cells between formulations with and without cholesterol (Fig. 6a) but there was variation in the mean fluorescence intensity (Fig. 6b), indicating that cells transfected with the cholesterol-containing nanocomplex produced more eGFP.

Further comparisons were performed with C14, C16 and C18 formulations with Pep 35, with and without cholesterol, analysed by fluorescence microscopy but likewise there were no significant differences in transfection efficiency in terms of cell numbers (Fig. S6).

We next investigated the relationship between mRNA uptake and transfection efficiency, by incorporating a Cy5-tagged mRNA into the

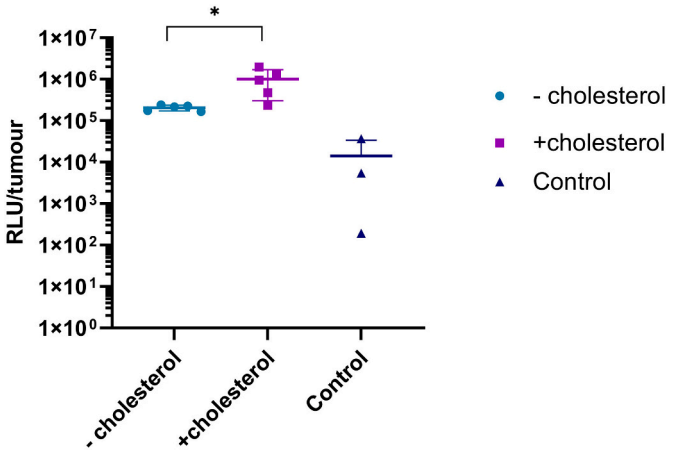

Fig. 5. Cholesterol formulations led to higher levels of protein expression compared to non-cholesterol formulations *in vivo*. C14/DOPE-Pep 35 (Screen A) or C14/DOPE+30% chol-Pep 35 (Screen B) nanocomplexes were injected into B16-F10 tumours of female C57BL/6 J mice. Luciferase expression was normalised to tumour mass. Controls were untransfected mice. Data are presented as mean ± SEM (n = 5 for treated mice and n = 3 for untreated control mice).

nanocomplex formulations. Cells were incubated with the nanocomplexes for between 30 min and 24 h, then fixed and imaged by confocal microscopy. 100% of B16-F10 and CT26 cells were positive for Cy5 fluorescence within 1 h for all formulations (Fig. 7a, b). A similar pattern was observed in H358 cells (Fig. 7c), although a lower number of Cy5-positive cells were observed with cholesterol-containing nanocomplexes. A reduction in fluorescence over time was observed in all transfections with fluorescence decreasing more rapidly in cholesterol-containing formulations than in cholesterol-free systems. This was particularly pronounced in B16-F10 cells, where only 40% of the cells transfected with C14/DOPE+30%Chol-Peptide 35 formulations were positive for Cy-5 puncta after 6 h incubation, compared to 80% for the same formulation without cholesterol. Although there were no significant differences in the number of cells taking up Cy5-labelled mRNA, the mean Cy5 fluorescence intensity within all cell types was significantly lower for nanocomplexes containing cholesterol (Fig. 7d–f). This reduced cellular intensity from Cy5 mRNA nanocomplexes containing cholesterol may be due to degradation, or more likely, since they generate enhanced transfection, may be due to better endosomal escape, and thus reducing intensity as they diffuse through the cytoplasm.

Confocal microscopy images at 1 h after transfection showed that Cy5 fluorescence from nanocomplex formulations with and without

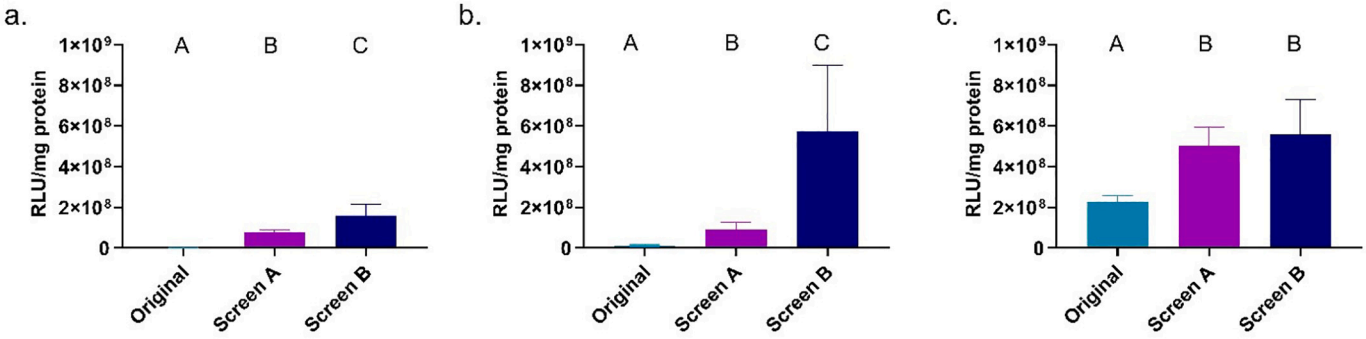

Fig. 4. The optimised formulations can transfect a range of cancer cells more efficiently than the original lipid-peptide system. Comparison of luciferase transfection efficiency of the 'Original' formulation (C14/DOPE-Pep 27) compared to the optimal screen A (C14/DOPE-Pep35) and optimal screen B (C14/DOPE+30%chol-Pep 35) nanocomplexes with 100 ng mRNA in; a) B16-F10 cells, b) CT26 cells, and c) NCI-H358 cells. Formulations which share a letter are not significantly different whilst those which do not are considered significantly different ($p < 0.05$) based on a one-way ANOVA test with Tukey post-hoc analysis. Data are presented as mean ± SEM, n = 6.

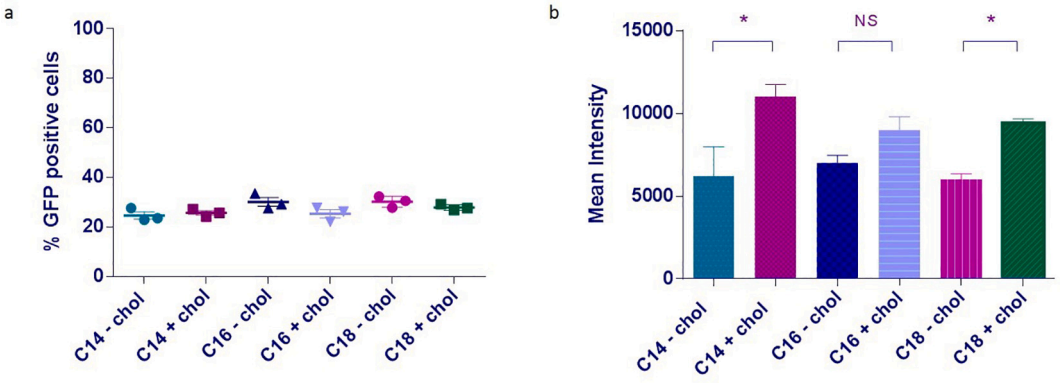

Fig. 6. Cholesterol formulations led to higher protein expression within individual cells but do not transfect a higher proportion of cells. Transfection efficiency in B16-F10 cells 24 h after delivery of 100 ng EGFP mRNA was measured by flow cytometry to determine, a) the percentage of eGFP positive cells after transfection, and b) average intensity of EGFP positive cells following transfection. Significant differences ($p < 0.05$) are denoted using an asterisk, based on a one-way ANOVA test with Tukey post-hoc analysis. Data are presented as mean ± SEM, $n = 6$.

cholesterol was mainly located in very small puncta (Fig. 7g), consistent with the size and distribution of early endosomes [20], although this was most easily seen with nanocomplexes without cholesterol. Images from later timepoints show Cy5 mainly in larger puncta that are generally closer to the cell nucleus, consistent with being in endolysosomes.

3.6. Biophysical properties with potential to enhance transfection

Having observed improvements in transfection efficiency with the addition of cholesterol *in vivo* and *in vitro,* we hypothesised that this could be due to increased extracellular stability of the nanocomplex, leading to increased protection of the mRNA from environmental RNAses, which are abundant in biological systems, or from increased potential of the cholesterol-containing nanoformulation to dissociate once within the cell [21]. Nanocomplexes were incubated with RNAse prior to transfection. The formulations without RNase treatment, displayed enhanced transfection from original formulation to screen A to Screen B A consistent with results shown in Fig. 4, while each formulation displayed decreases in transfection after RNase treatment, but these were not statistically significant (Fig. 8a). This suggests that differences in RNase protection are unlikely to be major factors in enhancing the transfection efficiency from Original to Screen A, to Screen B formulations.

We then explored whether improvements in the nanocomplexes could be explained by different dissociation capabilities in the presence of heparan sulphate, an anionic reagent. Formulations with transfection rankings C18/DOPE-Pep 27 < C14/DOPE-Pep 35 < C14/DOPE+30% chol–Pep 35 (Fig. 2) were compared in agarose gel electrophoresis experiments after incubation with heparin (Fig. 8b). Results indicated that all three formulations quenched fluorescence while all three were equally readily dissociated by heparin, with most mRNA migrating like the mRNA control samples. Heparin incubation had no direct effect on mRNA itself. These results reflect a similar capacity of all formulations to dissociate within the cell, and, therefore, that dissociation potential does not underpin transfection differences.

3.7. The effect of cholesterol on nanocomplex storage stability

A critical requirement for a pharmaceutical mRNA delivery system is stability on storage. The stability of nanocomplexes was investigated over a period of 28 days when stored at 4 °C. Size, surface charge, mRNA complexation efficiency and transfection efficiency was measured over this period (Fig. 9).

Screen A and Screen B formulations were similar in size on formulation on day 0, at approximately 150 nm and slightly smaller than the less efficient C14/DOPE-Pep 27 formulation at approximately 180 nm (Fig. 9a). No significant changes in size were observed over the 28-day duration of the study in the lead delivery system identified in screen B, C14/DOPE+30%chol-Pep 35 while a substantial size increase was observed of both C14/DOPE-Pep 27 and the optimal formulation from screen A, C14/DOPE-Pep 35 (Fig. 9a). Size and PDI measurements showed that cholesterol-containing complexes were more stable upon storage at 4 °C for up to 4 weeks, whereas complexes without cholesterol gradually increased to double their original size by day 28. Zeta potential values increased in the first 5 days for Screen A and B formulations but were stable thereafter (Fig. 9b). The improved stability of cholesterol-containing complexes was also demonstrated by their higher levels of mRNA complexation after 28 days of storage compared to the non-cholesterol formulations (Fig. 9c). High levels of complexation were achieved for all formulations at the start, but this decreased over time for formulations without cholesterol from over 90% to less than ~80% after 28 days while mRNA complexation efficiency of the cholesterol-containing formulations, remained unchanged for at least 28 days of storage.

The transfection efficiency of nanocomplexes after storage was assessed in B16-F10 melanoma cells (Fig. 9d). The efficacy of all complexes was reduced upon storage, but the reduction in transfection was markedly higher with complexes lacking cholesterol. The cholesterol-containing formulations retained their activity for 14 days followed by a gradual reduction. Thus, on storage, the optimised screen B formulation (C14/DOPE+30%chol-Pep35) displays improved storage stability and transfection efficiency, which seems to be a benefit of including cholesterol, and there may be further scope to enhance storage by freezing or freeze-drying.

3.8. IL-15 transfection

We finally assessed expression of IL-15 from transfected murine IL-15 mRNA, which has potential as a cancer therapy by cytokine adjuvant immunotherapy [22]. B16-F10 cells were transfected with nanocomplexes containing either murine IL-15 mRNA, or left untransfected in negative controls, then medium collected at 72 h and IL-15 protein quantified by ELISA (Fig. 10). Protein expression efficiency with the different nanocomplexes reflected the luciferase expression data with formulations ranking Screen B > Screen A > Original.

3.9. Discussion

In vitro transcribed mRNA offers a wide range of possibilities in the development of new therapeutics including vaccines for infectious diseases such as COVID-19, cancer vaccines and protein replacement therapies in genetic diseases. One of the major technical barriers to the

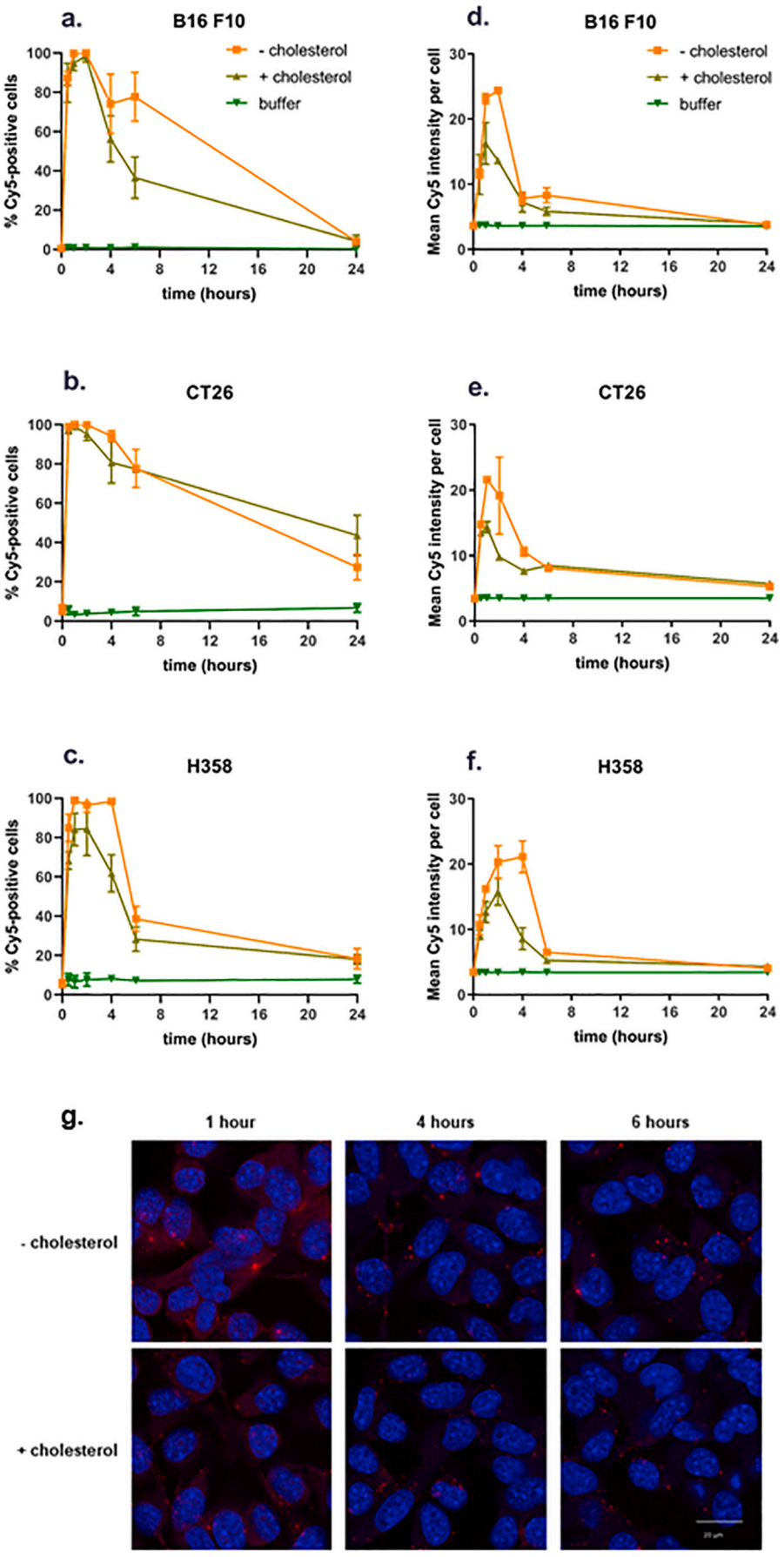

Fig. 7. Cellular uptake and transfection efficiency of Cy5 labelled mRNA (a-c) Percentage of cells displaying Cy5 fluorescence over 24 h and (d-f) mean fluorescence intensity per cell after incubation with cholesterol-containing and cholesterol-free nanocomplexes (Cy5-mRNA dose 1 μg/mL; mean and standard deviation), (g) Representative images of B16-F10 cells incubated for the indicated time with nanocomplexes formulated with or without cholesterol. Fixed cells were imaged at 60× magnification, scale bar 20 μm. Cell nuclei (blue) and Cy5-labelled mRNA (red). (For interpretation of the references to colour in this figure legend, the reader is referred to the web version of this article.)

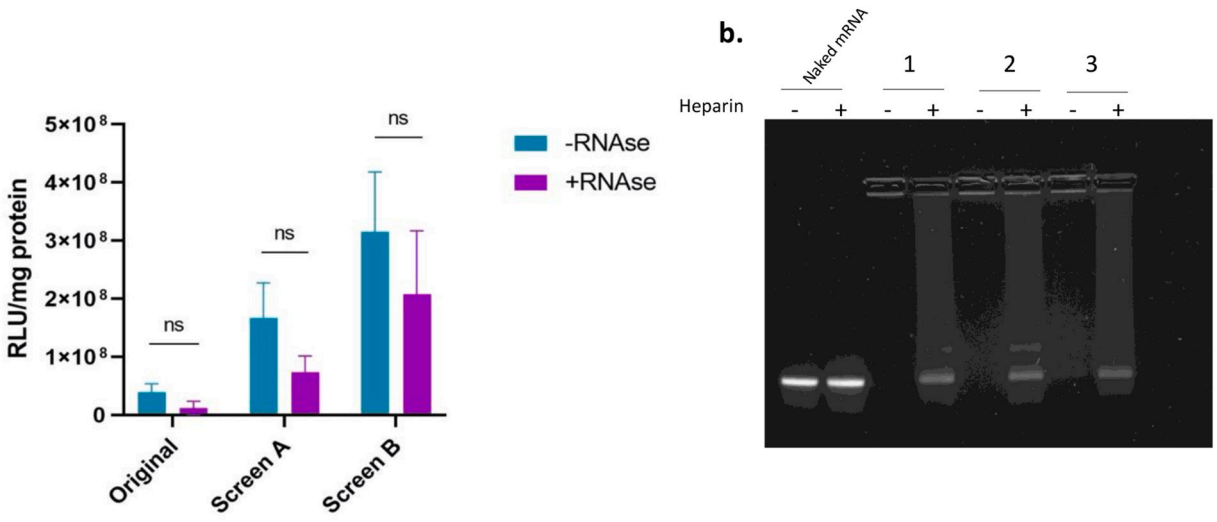

Fig. 8. Stability of Lipid-peptide nanocomplexes to RNAse and heparin.
a) RNase protection studies were carried out by measuring transfection with 100 ng of luciferase mRNA in B16-F10 cells with complexes treated with RNAse. Original formulation (C14/DOPE-Pep 27) was compared to the Screen A optimal (C14/DOPE-Pep 35) and Screen B optimal (C14/DOPE+30%chol-Pep 35) formulations. Differences between RNAse-free and RNAse-treated complexes are not significant according to a one-way ANOVA test with Tukey post-hoc analysis. Data are presented as mean ± SEM, $n = 6$; b) Stability of nanocomplexes incubated with (+) or without (−) heparin was compared by agarose gel electrophoresis, stained with ethidium bromide. The lanes on the gel from left to right are; Naked mRNA, Lane 1: C18/DOPE-Pep 27, lane 2: C14/DOPE-Pep 35 and lane 3: C14/DOPE-Pep 35+30% cholesterol.

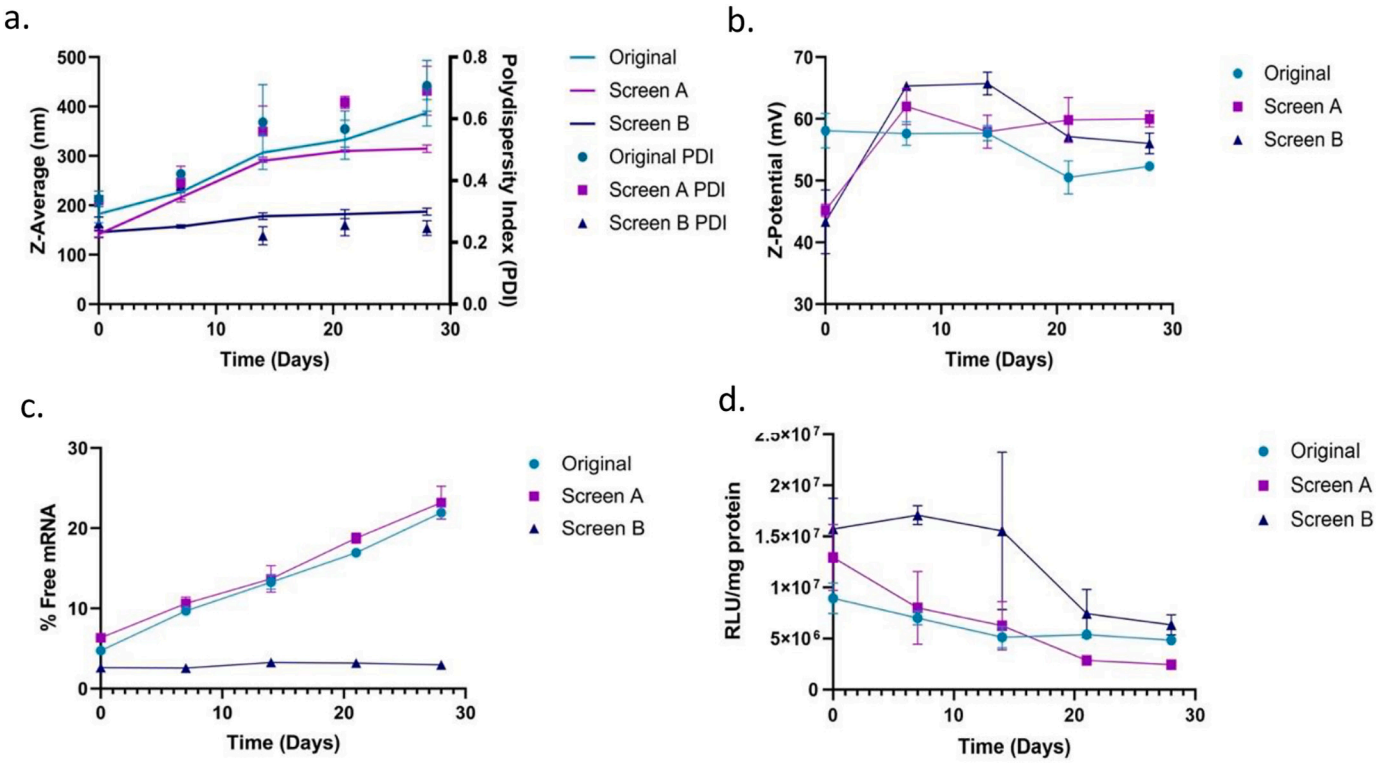

Fig. 9. Cholesterol formulations are more stable than their non-cholesterol counterparts, resisting changes in size, mRNA complexation and transfection efficiency over time. Stability characterisation of nanocomplexes after storage at 4 °C comparing "Original" formulation (C14/DOPE-Pep 27) with "Screen A" optimal (C14/DOPE-Pep 35) and "Screen B" optimal (C14/DOPE+30%chol-Pep 35) formulations showing, a) size variation and polydispersity index by DLS, b) zeta-potential by DLS, c) complexation stability measured by a RiboGreen quenching assay, and d) transfection efficiency with 100 ng luciferase mRNA, measured in B16-F10 cells in a luciferase assay.

realisation of this potential is the ability to efficiently package and deliver mRNA. Non-viral, nanoparticle technologies offer a solution to this problem but there are few formulations that are specifically optimised for mRNA delivery. We hypothesised that an optimised delivery system for mRNA might be developed from nanocomplex formulations that have proven effective for siRNA and pDNA delivery but that they would require significant development owing to the differing biochemical and biophysical properties of the different nucleic acids.

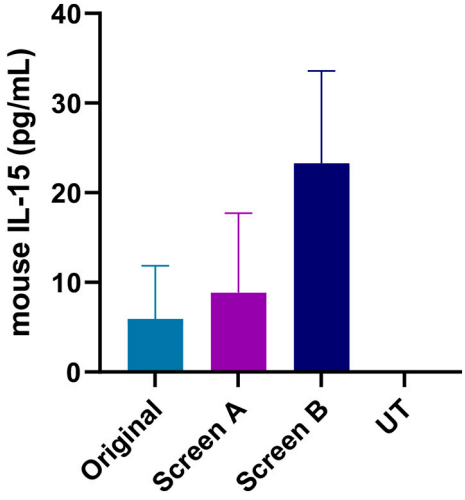

Fig. 10. Murine IL-15 mRNA transfection of B16-F10 cells. B16-F10 cells were transfected with 100 ng murine IL-15 mRNA comparing Original (C14/DOPE-Pep 27), Screen A (C14/DOPE-Pep 35) and Screen B (C14/DOPE+30% chol-Pep 35) formulations. IL-15 secreted into the medium was assayed by ELISA at 72 h after transfection. Data are presented as mean + SEM. $n = 3$. UT = untransfected cells.

In this study, we have optimised a lipid-peptide nanocomplex formulation similar to those used previously for pDNA [16] and siRNA delivery [14], for the delivery of mRNA by a multifactorial screening process. This approach resulted in three major improvements in the transfection efficiency of the lipid-peptide formulation. These were, 1) order of mixing improved by adding peptide last, *i.e.* RLP or LRP, 2) substituting peptide 27 (K_{16}RVRRGACRGDCL), which contains -an 'RGD' integrin-targeting peptide and 'RVRR' cleavable linker [17] for peptide 35 (K_{16}RVRRXSXGACYGLPHKFCG) which contains an improved targeting motif (YGLPHKF) identified previously by phage peptide library biopanning [15], and a hydrophobic motif 'XSX', in addition to the 'RVRR' cleavable linker, which resulted in an 8-fold transfection efficiency improvement, and 3), addition of cholesterol at 30% of total lipid, which resulted in a further 5-fold improvement. This supports our hypothesis that optimised delivery systems for siRNA and DNA differ significantly from those for mRNA and so we then progressed to optimise variables and to determine why these alterations had such beneficial effects.

First, we found that the optimal order of mixing involved adding the peptide last, which may impact on the position of the peptide on the nanocomplex during formulation. Possibly, adding the peptide last results in the peptide having greater exposure at the surface and a greater impact on targeting and uptake. Further physical characterisation of the location of the peptide on the surface is necessary to confirm this.

For the first multifactorial screen (screen A), we explored varying alkyl chain lengths of the cationic lipids since we have shown previously that this is an important variable for pDNA delivery in epithelial cells [23]. Other studies have also shown that there is a range of effective designs, such as the lipidoid materials C12–200 [24], 503,013 [19], cKKe12 [11], OF-02 [25] with tail lengths of 12, 13, 10, 18, respectively. Lipids more like those developed in this work have been reported such as the DLin-DMA family of ionizable lipids [26,27]. DLin-MC3-DMA [28] was recently the first approved LNP based siRNA drug by Alnylam Pharmaceuticals [29]. This lipid contains C18 tails, while, interestingly, in the evolution of these type of lipids, it has been mainly alterations to the head group driving improvements. Previous reports indicate that there is no universal optimal lipid tail length design, and that empirical optimisation is required specific for the formulation type and the application in relation to target cells and nucleic acid cargo. We found in this study that the C14 lipid was the most potent in lipid-peptide formulations.

The phospholipids, DSPC, DOPE and DOPC, also evaluated in screen A, may help mediate endosomal release and provide structural stability as previously reported for pDNA nanocomplexes [10,30], and lipoplexes [31]. DOPE was optimal followed by DOPC then DSPC due, presumably, to the fusogenic effects of DOPE [30]. Phospholipids with large headgroups and saturated hydrocarbon chains adopt a more cylindrical structure, which results in the nanocomplexes produced being very stable owing to the lipids' ability to form tightly packed bilayer membranes which could restrict mRNA release. The DSPC structure is the most cylindrical of the phospholipids tested, hence it may be that mRNA release was restricted in these formulations, resulting in its lower transfection efficiencies. DOPE has a smaller headgroup as well as unsaturated chains giving rise to a 'kink' in the tail, is conical in structure and may, therefore, form less stable lipid membrane [33]. resulting in easier release of mRNA from the DOPE-containing systems. The structure of DOPC is intermediate between the two other phospholipids. Although it has the larger choline headgroup, the presence of the partially unsaturated chain alters its properties from DSPC. The superiority of DOPE over DOPC is in accordance with previous findings where the two were tested in lipid-peptide complexes to deliver pDNA to a bronchial epithelial cell line [31]. The impact of the helper lipid has also been shown to be heavily influenced by the other components in a delivery system. For example, the lipidoid formulations C12–200 [24] and CkkE12 [11] all found DOPE to be more potent than DSPC, although, for the MC3-like lipids, DSPC was the optimal phospholipid for siRNA delivery. Interestingly, when this system was adapted for pDNA delivery, DOPE was found to be more potent than DSPC [32], thus demonstrating that the optimal helper lipid for a given transfection formulation is determined by the combination of components in it.

The most important component for improvement in transfection efficiency in screen A was the peptide. Three peptides were compared, that each shared the same oligolysine domain (K_{16}) for mRNA electrostatic interactions and packaging, and a cyclic targeting motif (CYGLPHKFC) [15]. The peptide hydrophobic region in the linker XSX, where X is epsilon-amino hexanoic acid, may promote extracellular stability of the nanocomplex, protecting the mRNA from environmental nucleases, while the cleavable region of the linker may, in contrast, promote intracellular disassembly, enabling availability and accessibility of mRNA to the translational machinery [10,13,16]. Cleavage of the RVRR linker by the endosomal enzymes furin and cathepsin B separates the targeting ligand from the intact nanocomplex in the endosome, detaching it from the receptor, and so promoting trafficking to the cytoplasm. The optimal peptide (Peptide 35), which resulted in an 8-fold improvement over Peptide 28, contained the same targeting motif but with the addition of the hydrophobic and cleavable peptide motifs.

The second phase of our screening strategy focused on incorporating cholesterol into the formulation. Cholesterol may enhance particle stability and protection of the mRNA [33], as well as promoting fusion with endosomal membranes enabling endosomal release, both of which improve transfection efficiency [17,34]. In a detailed imaging study, lipid-based nanoparticles (LNPs) *in vitro* and *in vivo* showed endosomal escape efficiencies of only 1–2% of siRNA, highlighting the barrier this presents [35]. The addition of cholesterol to the lipid-peptide formulations led to an increase in transfection efficiency both *in vitro* and *in vivo* which we hypothesised was a result of enhanced endosomal release. Fluorescence microscopy and flow cytometry experiments showed little difference between formulations in mRNA uptake (Fig. 7), or the number of cells transfected (Fig. 6). However, we observed a comparatively rapid reduction after transfection in Cy5-mRNA-positive puncta in confocal images, with the cholesterol containing formulations, indicating enhanced endosomal escape. Loss of Cy5 puncta may also be attributed to Cy5-mRNA degradation or recycling of mRNA out of the cell but either of these would be expected to reduce transfection efficiency rather than the enhancement observed [36,37]. These findings are consistent with cholesterol facilitating escape from intracellular

vesicles early in the endocytic process. In studies of stability of nanocomplexes on storage at 4 °C, cholesterol-containing formulations were much better than cholesterol-free formulations, regarding size and packaging efficiency. Thus, improved transfection efficiency of the cholesterol containing nanocomplex formulations may be explained by improved stability, in addition to enhanced intracellular trafficking.

Further attempts to optimise the lipid-peptide delivery system by increasing the ratios of lipid and peptide to mRNA (Fig. S4) led to increased toxicity, due possibly to increased net charge or non-complexed lipid and peptide components as previously reported [38–40], for example by damaging the cell membrane [41], and so this route was not pursued further.

Studies were performed to determine the potential of this formulation for pharmaceutical development. Cholesterol containing formulations exhibited the best stability profile with respect to size and complexation efficiency which remained unchanged for 28 days (Fig. 9). This may be explained by enhanced membrane rigidity imparted by cholesterol, allowing the nanocomplexes to resist breakdown or aggregation [34,42]. Although particle characteristics did not change over 28 days, transfection efficiency decreased significantly after 14 days. The characterisation approaches used in this study do not account for internal changes occurring in the particle. Factors such as internal reorganisation of the particle structure or mRNA degradation may not affect particle size or complexation but still may impact transfection efficiency. More advanced analytical characterisation such as neutron scattering techniques demonstrated by others are needed to understand this further [43].

The cholesterol – containing formulation displayed better transfection than the cholesterol-free nanocomplex *in vivo* after direct injection into syngeneic tumours of B16-F10 in C57Bl/6 J mice. Intratumoural delivery offers many therapeutic routes and has been described for testing mRNA cancer therapeutics [44]. IL-15 has long been proposed as an immunotherapy for cancers by activating natural killer (NK) cells, B cells and T cells, and increasing the production of cytokine-like tumour necrosis factor-alpha (TNF-α) and interferon-gamma (IFN-γ) [22, 46]. The nanocomplex formulation transfected successfully B16-F10 cells *in vitro* with IL-15 mRNA, thus, illustrating the potential of this formulation which will now be investigated *in vivo* by direct intratumoural delivery as well as by intravenous delivery although we may need to include PEGylated lipids in the mRNA formulation for systemic delivery.

3.10. Conclusions

A delivery system initially designed for siRNA and DNA delivery, has been optimised for mRNA delivery. We have demonstrated significant improvements in the mRNA transfection efficiency, achieved by the addition of an improved targeting peptide and incorporating cholesterol into the formulation which improved both particle stability as well as endosomal escape. The multi-factorial approach to optimisation revealed that the phospholipid DOPE was critical to the performance of the lipid-peptide formulation, whereas altering the cationic lipid tail length had minimal impact. Furthermore, the mRNA formulation was shown to have promising pharmaceutical development properties maintaining stability and transfection efficiency for at 4 °C. We also demonstrated that this system has minimal cytotoxicity and is effective for *in vivo* transfection of tumours. Delivery of IL-15 mRNA *in vitro* was demonstrated and, thus, a pathway to developing cancer therapies. In summary, this study provides evidence of a new potent delivery system for potential therapeutic use in the delivery of mRNA.

Author contributions

D. Grant-Serroukh performed most of the experiments, analysed most of the data, and drafted the manuscript. R. Maeshima performed the heparin-release, gel retardation and IL-15 mRNA study and analysed the data. M. R. Hunter designed and performed confocal imaging experiments and carried out analysis of this data. A. Tagalakis and A. Aldossary performed the *in vivo* experiments, and A.Tagalakis processed the tumour samples and performed and analysed the relevant luciferase assays. N. Allahham performed data analysis and prepared figures for the manuscript. S. Hart provided project supervision, while S. Hart, A. Desai, M. Edbrooke and G. Williams reviewed data and design of the experiments. All authors provided input into the manuscript and analysis of experimental results.

Credit author statement

Conception or design of the work: Mark Edbrooke, Arpan Desai and Stephen L. Hart.

Project supervision: Gareth R. Williams and Stephen L. Hart.

Data collection: Dania Grant-Serroukh, Morag R. Hunter, Ruhina Maeshima, Aristides D. Tagalakis, Ahmad M. Aldossary, Nour Allahham,

Data analysis and interpretation: Dania Grant-Serroukh, Morag R. Hunter, Ruhina Maeshima, Mark Edbrooke, Arpan Desai and Stephen L. Hart.

Drafting the article: Dania Grant-Serroukh, Gareth R. Williams and Stephen L. Hart.

Critical revision of the article: Aristides D. Tagalakis, Morag R. Hunter, Mark Edbrooke, Arpan Desai.

Final approval of the version to be published: Dania Grant-Serroukh, Morag R. Hunter, Ruhina Maeshima, Aristides D. Tagalakis, Ahmad M. Aldossary, Nour Allahham' Gareth R. Williams, Mark Edbrooke, Arpan Desai, and Stephen L. Hart.

Declaration of Competing Interest

None.

Acknowledgments

DG was funded by the Engineering and Physical Sciences Research Council (EPSRC) Centre of Doctoral Training (CDT) in Advanced Therapeutics and Nanomedicine (EP/L01646X). These studies were supported by the National Institute for Health Research Biomedical Research Centre at Great Ormond Street Hospital for Children NHS Foundation Trust and University College London. MRH is a fellow of the AstraZeneca postdoctoral programme and NA was supported through the EPSRC & SFI CDT in Transformative Pharmaceutical Technologies (EP/S023054/1).

Appendix A. Supplementary data

Supplementary data to this article can be found online at https://doi.org/10.1016/j.jconrel.2022.06.018.

References

[1] U. Sahin, K. Kariko, O. Tureci, mRNA-based therapeutics–developing a new class of drugs, Nat. Rev. Drug Discov. 13 (10) (2014) 759–780.
[2] K.S. Corbett, et al., SARS-CoV-2 mRNA vaccine design enabled by prototype pathogen preparedness, Nature 586 (7830) (2020) 567–571.
[3] J.D. Gillmore, et al., CRISPR-Cas9 in vivo gene editing for transthyretin amyloidosis, N. Engl. J. Med. 385 (6) (2021) 493–502.
[4] D. Haussecker, Stacking up CRISPR against RNAi for therapeutic gene inhibition, FEBS J. 283 (17) (2016) 3249–3260.
[5] J. Kaiser, Gene editor injected into the body treats disease, Science 373 (6550) (2021) 16.
[6] M.P. Stewart, R. Langer, K.F. Jensen, Intracellular delivery by membrane disruption: mechanisms, strategies, and concepts, Chem. Rev. 118 (16) (2018) 7409–7531.
[7] P. Midoux, C. Pichon, Lipid-based mRNA vaccine delivery systems, Exp. Rev. Vaccines. 14 (2) (2015) 221–234.
[8] K.J. Kauffman, M.J. Webber, D.G. Anderson, Materials for non-viral intracellular delivery of messenger RNA therapeutics, J. Control. Release 240 (2016) 227–234.

[9] U. Lachelt, E. Wagner, Nucleic acid therapeutics using polyplexes: a journey of 50 years (and beyond), Chem. Rev. 115 (19) (2015) 11043–11078.
[10] M.M. Munye, et al., Role of liposome and peptide in the synergistic enhancement of transfection with a lipopolyplex vector, Sci. Rep. 5 (2015) 9292.
[11] Y. Dong, et al., Lipopeptide nanoparticles for potent and selective siRNA delivery in rodents and nonhuman primates, Proc. Natl. Acad. Sci. U. S. A. 111 (11) (2014) 3955–3960.
[12] K.J. Kauffman, et al., Optimization of lipid nanoparticle formulations for mRNA delivery in vivo with fractional factorial and definitive screening designs, Nano Lett. 15 (11) (2015) 7300–7306.
[13] A.D. Tagalakis, et al., Integrin-targeted nanocomplexes for tumour specific delivery and therapy by systemic administration, Biomaterials 32 (5) (2011) 1370–1376.
[14] A.D. Tagalakis, et al., Receptor-targeted liposome-peptide nanocomplexes for siRNA delivery, Biomaterials 32 (26) (2011) 6302–6315.
[15] M.J. Writer, et al., Targeted gene delivery to human airway epithelial cells with synthetic vectors incorporating novel targeting peptides selected by phage display, J. Drug Target. 12 (4) (2004) 185–193.
[16] S.M. Grosse, et al., Tumor-specific gene transfer with receptor-mediated nanocomplexes modified by polyethylene glycol shielding and endosomally cleavable lipid and peptide linkers, FASEB J. 24 (7) (2010) 2301–2313.
[17] A. Zidovska, et al., The role of cholesterol and structurally related molecules in enhancing transfection of cationic liposome-DNA complexes, J. Phys. Chem. B 113 (15) (2009) 5208–5216.
[18] K. Paunovska, et al., A direct comparison of in vitro and in vivo nucleic acid delivery mediated by hundreds of nanoparticles reveals a weak correlation, Nano Lett. 18 (3) (2018) 2148–2157.
[19] K.A. Whitehead, et al., Degradable lipid nanoparticles with predictable in vivo siRNA delivery activity, Nat. Commun. 5 (2014) 10.
[20] D.C. Lawe, et al., The FYVE domain of early endosome antigen 1 is required for both phosphatidylinositol 3-phosphate and Rab5 binding. Critical role of this dual interaction for endosomal localization, J. Biol. Chem. 275 (5) (2000) 3699–3705.
[21] L. Parnaste, et al., The formation of nanoparticles between small interfering RNA and amphipathic cell-penetrating peptides, Mol. Ther. Nucleic Acids. 7 (2017) 1–10.
[22] S. Lei, et al., Efficient colorectal cancer gene therapy with IL-15 mRNA nanoformulation, Mol. Pharm. 17 (9) (2020) 3378–3391.
[23] M. Writer, et al., Analysis and optimization of the cationic lipid component of a lipid/peptide vector formulation for enhanced transfection in vitro and in vivo, J. Liposome. Res. 16 (4) (2006) 373–389.
[24] K.T. Love, et al., Lipid-like materials for low-dose, in vivo gene silencing, Proc. Natl. Acad. Sci. U. S. A. 107 (5) (2010) 1864–1869.
[25] O.S. Fenton, et al., Bioinspired alkenyl amino alcohol ionizable lipid materials for highly potent in vivo mRNA delivery, Adv. Mater. 28 (15) (2016) 2939–2943.
[26] S.C. Semple, et al., Rational design of cationic lipids for siRNA delivery, Nat. Biotechnol. 28 (2) (2010) 172–176.
[27] J. Heyes, et al., Cationic lipid saturation influences intracellular delivery of encapsulated nucleic acids, J. Control. Release 107 (2) (2005) 276–287.
[28] M. Jayaraman, et al., Maximizing the potency of siRNA lipid nanoparticles for hepatic gene silencing in vivo, Angew. Chem. Int. Ed. Eng. 51 (34) (2012) 8529–8533.
[29] P.R. Cullis, M.J. Hope, Lipid nanoparticle systems for enabling gene therapies, Mol. Ther. 25 (7) (2017) 1467–1475.
[30] M.A. Oberli, et al., Lipid nanoparticle assisted mRNA delivery for potent cancer immunotherapy, Nano Lett. 17 (3) (2017) 1326–1335.
[31] Z. Du, et al., The role of the helper lipid on the DNA transfection efficiency of lipopolyplex formulations, Sci. Rep. 4 (2014) 7107.
[32] J.A. Kulkarni, et al., Design of lipid nanoparticles for in vitro and in vivo delivery of plasmid DNA, Nanomedicine 13 (4) (2017) 1377–1387.
[33] K.A. Hajj, K.A. Whitehead, Tools for translation: non-viral materials for therapeutic mRNA delivery, Nat. Rev. Mater. 2 (2017).
[34] J.L. Betker, et al., Cholesterol domains enhance transfection, Ther. Deliv. 4 (4) (2013) 453–462.
[35] J. Gilleron, et al., Image-based analysis of lipid nanoparticle-mediated siRNA delivery, intracellular trafficking and endosomal escape, Nat. Biotechnol. 31 (7) (2013) 638–646.
[36] C. Alabi, A. Vegas, D. Anderson, Attacking the genome: emerging siRNA nanocarriers from concept to clinic, Curr. Opin. Pharmacol. 12 (4) (2012) 427–433.
[37] Martens, T., et al., Intracellular delivery of nanomaterials: how to catch endosomal escape in the act. Nano Today 9(3).
[38] E. Frohlich, The role of surface charge in cellular uptake and cytotoxicity of medical nanoparticles, Int. J. Nanomedicine 7 (2012) 5577–5591.
[39] A. Lechanteur, et al., PEGylation of lipoplexes: the right balance between cytotoxicity and siRNA effectiveness, Eur. J. Pharm. Sci. 93 (2016) 493–503.
[40] L. Shang, K. Nienhaus, G.U. Nienhaus, Engineered nanoparticles interacting with cells: size matters, J. Nanobiotechnol. 12 (2014) 5.
[41] J.Q. Lin, et al., A simulation study on nanoscale holes generated by gold nanoparticles on negative lipid bilayers, Langmuir 27 (13) (2011) 8323–8332.
[42] J. Senior, G. Gregoriadis, Stability of small unilamellar liposomes in serum and clearance from the circulation: the effect of the phospholipid and cholesterol components, Life Sci. 30 (24) (1982) 2123–2136.
[43] M. Yanez Arteta, et al., Successful reprogramming of cellular protein production through mRNA delivered by functionalized lipid nanoparticles, Proc. Natl. Acad. Sci. U. S. A. 115 (15) (2018) E3351–E3360.
[44] J.Q. Liu, et al., Intratumoral delivery of IL-12 and IL-27 mRNA using lipid nanoparticles for cancer immunotherapy, J. Control. Release 345 (2022) 306–313.